Available online at www.sciencedirect.com
ScienceDirect
Polymer 48 (2007) 7309–7315
polymer
www.elsevier.com/locate/polymer

Immobilization of antioxidant on nanosilica and the antioxidative behavior in low density polyethylene

Xiaowei Gao, Guangjun Hu, Zhongzhong Qian, Yanfen Ding, Shimin Zhang,
Dujin Wang, Mingshu Yang*

Beijing National Laboratory for Molecular Sciences, Key Laboratory of Engineering Plastics, Institute of Chemistry,
Chinese Academy of Sciences, Beijing 100080, China

Received 10 May 2007; received in revised form 30 September 2007; accepted 12 October 2007

Abstract

Nanosilica was firstly modified with an aminosilane coupling agent (AEAPS) and then reacted with the reactive antioxidant, 3,5-di-*tert*-butyl-4-hydroxycinnamic acyl chloride (AO-Cl), to form a nanosilica-immobilized antioxidant, AO–AEAPS–silica. FT-IR, XPS and TGA measurements confirmed that the reactive antioxidant was chemically immobilized onto the nanosilica surface. SEM observation showed that the nanosilica-immobilized antioxidant was homogeneously dispersed into the matrix of low density polyethylene (LDPE). It has been found that the antioxidative efficiency of AO–AEAPS–silica was superior to the corresponding low molecular counterpart (AO), based on the measurement of the oxidation induction time (OIT) of the LDPE/AO–AEAPS–silica and the LDPE/AO compounds containing equivalent antioxidant component. The release of the antioxidant from LDPE films was evaluated by monitoring the OIT change upon water extraction, demonstrating that AO–AEAPS–silica retained high stability against migration.

Keywords: Silica; Antioxidative behavior; Low density polyethylene

1. Introduction

To extend the service life and enhance the performance of polymers for required applications, additives are usually added into polymers, such as antioxidants, light stabilizers, thermal stabilizers, fire retardants and antistatic agents. Hindered phenols are of the most prominent antioxidants and widely used in polyolefins. However, the use of low molecular weight phenol antioxidants is always restricted because of two drawbacks: (1) they are easy to volatilize at high temperature during polymer processing; (2) they have low resistance to migration and extraction during the long-term service. To overcome these drawbacks, high molecular weight counterparts, e.g. Irganox® 1010 and Irganox® 1076, were developed commercially. However, it was found that these high molecular weight antioxidants also suffered from physical loss to some extent by leaching out under aggressive service conditions [1–3]. Another method of accomplishing this objective is to immobilize the reactive antioxidants onto the polymer backbone or other solid supports. It was demonstrated that the extraction resistance of polymer grafted antioxidants dramatically improved [4,5].

Nanosilica has been widely used in polymers as inorganic filler to improve the properties of polymeric materials [6–17]. Over the last 10 years, nanosilica has served as a promising support material for designing and preparing new functional materials because of its high surface area and stability. For example, there has been much research on the modification of nanosilica with biomolecules to prepare sensors, medical diagnostics, antibody, etc [18–20]; several research groups [21–25] have also prepared silica-supported catalysts by immobilizing catalysts onto the surface of nanosilica particles. However, to the best of our knowledge, there have been no reports about immobilizing reactive antioxidants onto the

---

* Corresponding author. Tel./fax: +86 10 82615665.
E-mail address: yms@iccas.ac.cn (M. Yang).

0032-3861/$ - see front matter © 2007 Elsevier Ltd. All rights reserved.
doi:10.1016/j.polymer.2007.10.015

surface of nanosilica particles to prepare silica-immobilized antioxidants.

The aim of this work is to prepare a novel antioxidant using nanosilica as solid support to immobilize reactive antioxidant onto the surface. Hence, the chemical immobilization of reactive antioxidant onto the surface of nanosilica particles has been investigated. The antioxidative efficiency was evaluated by oxidative induction time (OIT) method. It has been revealed that the nanosilica-immobilized antioxidant retained excellent stability in LDPE matrix against water extraction. Therefore, this nanosilica-immobilized antioxidant is expected to be a new type of antioxidant with high performances such as non-volatile, non-migratory and not lost during the aggressive service life.

2. Experimental

2.1. Materials

Aerosil-200 fumed silica (surface area 200 ± 25 m^2/g, primary particle size 12 nm, purity 9.8%) was obtained from Degussa-Hüls, and dried in a vacuum oven overnight at 105 °C before use. The reactive antioxidant 3,5-di-*tert*-butyl-4-hydroxycinnamic acid (AO, purity 99.8%) was purchased from Alfa Aesar and used as-received. The aminosilane coupling agent *N*-(2-aminoethyl)-3-aminoproplytrimethoxysilane (AEAPS) was a commercial sample obtained from Hubei Wuhan University Silicon New Material Co, Ltd. The low density polyethylene, LDPE 1I2A, was supplied by Yanshan Petrochemical Co LTD, Beijng, China. The toluene and triethylamine were of analytical grade and used after distillation. All other solvents and reagents were used as-received.

2.2. Preparation of nanosilica-immobilized antioxidant

The synthesis route is shown in Scheme 1.

Fumed nanosilica (12.0 g) was dispersed in anhydrous toluene (400 mL). AEAPS (22.5 g) was added into the suspension. The mixture was refluxed under stirring for 24 h. The product was filtered and then washed with anhydrous toluene (400 mL, 3 times) and absolute ethanol (400 mL, 3 times). The functionalized nanosilica (AEAPS–silica) was dried in a vacuum oven overnight at 105 °C.

AO (2.5 g) was dissolved in thionyl chloride and the reaction mixture was allowed to reflux until no hydrochloric acid was generated. The obtained acyl chloride (AO-Cl) was added to the suspension of AEAPS–silica (6.0 g) in anhydrous toluene (200 mL) under stirring. Anhydrous triethylamine (10 mL) was next added drop wise and the mixture was stirred for 20 h at room temperature under nitrogen atmosphere. The product was filtered and washed with anhydrous toluene (200 mL, 3 times) and absolute ethanol (200 mL, 3 times). The nanosilica-immobilized antioxidant (AO–AEAPS–silica) was dried in a vacuum oven overnight at 105 °C.

2.3. Preparation of LDPE/silica nanocomposites

The LDPE/silica nanocomposites were prepared by melt compounding method using a HAAKE Rheomix-600 internal mixer (Mess-Technic GmbH, Germany) at 190 °C with a screw speed of 50 rpm for 5 min. Prior to the melt processing, the neat nanosilica and modified nanosilica were dried in a vacuum oven overnight at 105 °C. The content of inorganic component was fixed at 4 wt% in all samples of nanocomposites. The inorganic contents of the modified nanosilica were determined by the residues of thermogravimetric analysis up to 750 °C. Several LDPE compounds were prepared and their compositions are listed in Table 1. In the LDPE/AO blend, the AO content is 0.55 wt%, equivalent to the molar fraction of the antioxidant in LDPE/AO–AEAPS–silica nanocomposite. The prepared materials were pressed into sheets at 160 °C with an average thickness of 260 μm and saved for later extraction experiment and DSC test.

2.4. Extraction experiments

The obtained films (6 pieces per sample, 2 × 2 cm; thickness, 260 μm) of LDPE/AO and LDPE/AO–AEAPS–silica compounds were immersed in de-ionized water (500 mL) in a glass beaker. The extraction temperature was maintained at 45 °C by placing the beaker in a temperature controlled oil bath. At appropriate time intervals, the films were taken out from water and stored in desiccators for later DSC test. Extraction water was completely changed every 2 days. The release of the antioxidant from LDPE films was evaluated by monitoring the OIT change upon water extraction.

2.5. Characterization

Infrared spectra were recorded with KBr pellets on a Perkin–Elmer-System 2000 infrared spectrum analyzer in the wave number range of 4000–370 cm^{-1}. X-ray photoelectron spectroscopy (XPS) data were obtained with an ESCA-Lab220i-XL electron spectrometer from VG Scientific using 300 W Al Kα radiation. The base pressure is about 3×10^{-9} mbar. The binding energies are referenced to the C1s line at 284.6 eV from adventitious carbon. Perkin–Elmer TGA-7 was used to measure the thermal behavior of the modified silica in nitrogen atmosphere from 50 °C to 750 °C at a heating rate of 20 °C/min. Transmission electron microscope (TEM) images were obtained using a Hitachi (Japan) H-800 instrument with an accelerate voltage of 150 kV. Scanning electron microscope (SEM) images were taken on a JEOL S-4300F field emission scanning electron microscope at 5 kV. Oxidation induction time (OIT) measurement was performed on a Perkin–Elmer DSC 7 according to the standard method (ISO 11357-6, 2002), which specified the gas flow and temperature ramping. The method used for the OIT test proceeded as follows. Firstly, the sample was held at 60 °C for 5 min with a nitrogen flow of 50 mL/min. Subsequently, the sample was heated to 200 °C at a rate of 20 °C/min, still under a flow of nitrogen. After reaching

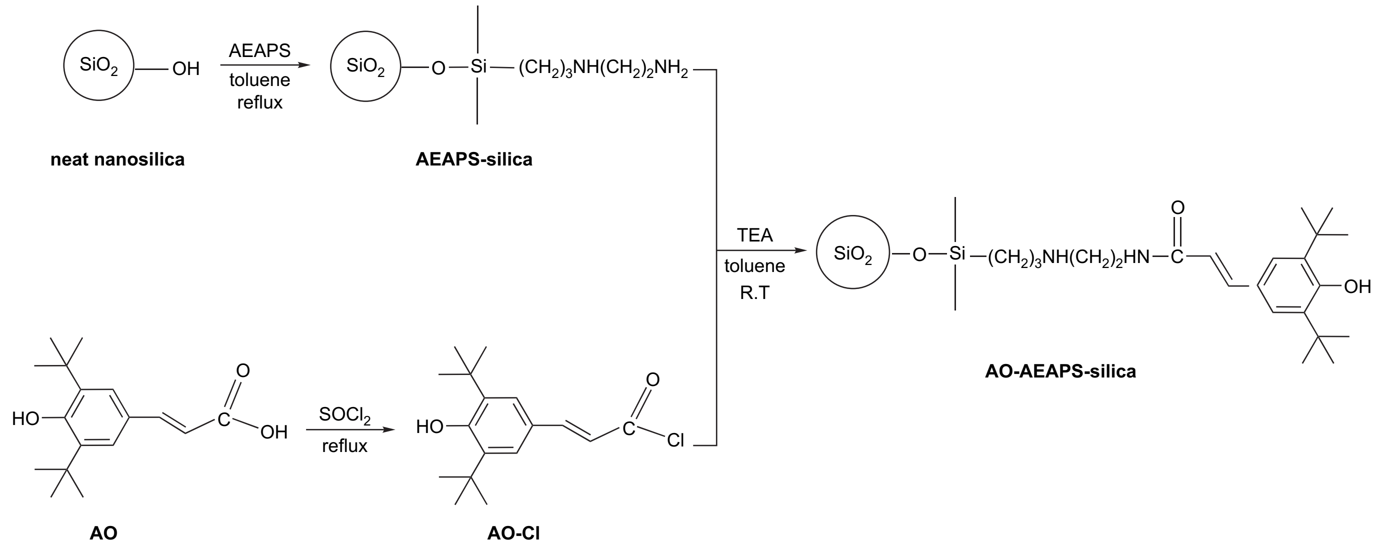

Scheme 1. Synthesis of AO–AEAPS–silica.

200 °C, the sample was held for another 5 min, at which point the gas was switched to oxygen at a flow rate of 50 mL/min. The oxidation of the sample was observed as a sharp increase in heat flow due to the exothermic nature of the oxidation reaction. The OIT was obtained by the software of Perkin–Elmer DSC 7.

3. Results and discussion

3.1. Immobilization of the reactive antioxidant onto the surface of nanosilica particles

The intention of this work is to create chemical bonding between the antioxidant molecules and the nanosilica particles. The antioxidant used here [3,5-di-*tert*-butyl-4-hydroxycinnamic acid (AO)], however, cannot directly react with nanosilica; hence the functionalization of nanosilica is needed. The nanosilica particles are hydrophilic and have many hydroxyl groups (–OH) on their surface that allow surface modification with various chemical species. So an aminosilane coupling agent, *N*-(2-aminoethyl)-3-aminoproplytrimethoxysilane (AEAPS), was used as the surface modifier of nanosilica. After functionalization, there are amino groups ($-NH_2$) on the surface of nanosilica that provide chemical linkages with the meanwhile chloro-acetylated antioxidant (AO-Cl). Scheme 1 illustrates the synthesis route of the nanosilica-immobilized antioxidant, AO–AEAPS–silica. Since the adsorbed water in nanosilica could annihilate acyl chloride groups, the route of direct reaction between nanosilica and the reactive antioxidant is not effective and thus was not used.

Table 1
LDPE compounds and their compositions

Sample	Type of additives	Content of additives (wt%)
Pure LDPE	–	–
LDPE/nanosilica	Neat nanosilica	4
LDPE/AEAPS–silica	AEAPS–silica	4.48
LDPE/AO–AEAPS–silica	AO–AEAPS–silica	5.06
LDPE/AO	AO	0.55

Fig. 1 shows the FT-IR spectra of neat nanosilica, AEAPS–silica and AO–AEAPS–silica. In the neat nanosilica, the broad strong bands around 3700–3200 cm^{-1} are assigned to the O–H stretching vibration of silanol hydroxyls and adsorbed water, while the absorption at 1630 cm^{-1} is assigned to the O–H bending of adsorbed water. In AEAPS–silica, the bands around 2935 cm^{-1} and 2870 cm^{-1} are attributed to CH_2 asymmetric and symmetric stretches, respectively, and the absorption at 1470 cm^{-1} is the characteristic of CH_2 bending. The shoulder absorption around 1570 cm^{-1} attributed to N–H bending is not clearly observed because of the low amine content of AEAPS on nanosilica and overlapping of broad strong absorption of hydrogen band around 1630 cm^{-1}. In AO–AEAPS–silica, absorption of the amide

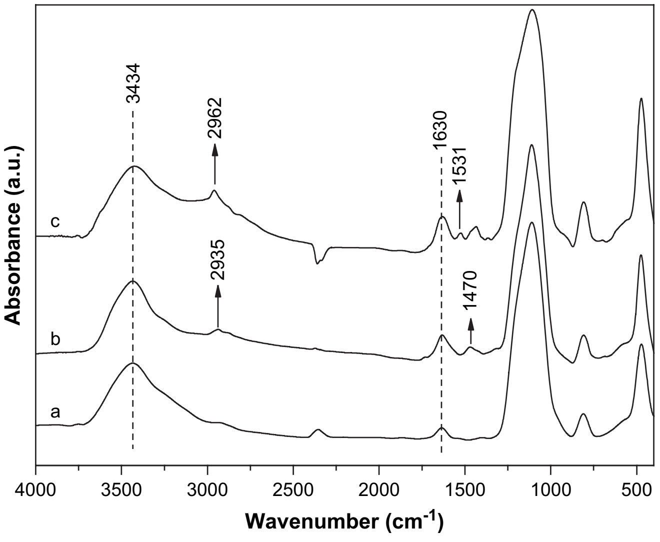

Fig. 1. FT-IR spectra of (a) neat nanosilica, (b) AEAPS–silica and (c) AO–AEAPS–silica.

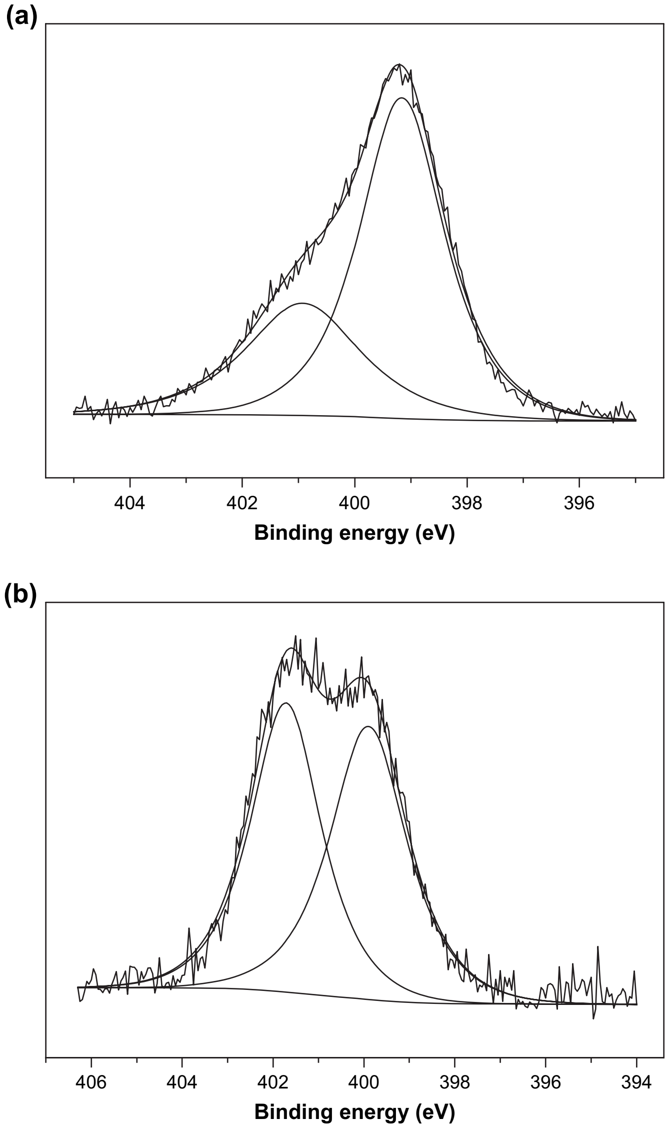

Fig. 2. XPS spectra of (a) AEAPS–silica and (b) AO–AEAPS–silica in the N1s region.

II at around 1531 cm^{-1} is noticeable, which confirms chemical reaction between the acyl chloride groups of reactive antioxidant and the $-NH_2$ groups on the AEAPS–silica surface. This result also indicates that the aminosilane coupling agent has been anchored onto the nanosilica surface after the functionalization of nanosilica. The absorption of amide I around 1660 cm^{-1} is not detected in the spectra of AO–AEAPS–silica because of the broad strong absorption of hydrogen band about 1630 cm^{-1}. Another obvious characteristic on AO–AEAPS–silica is the enhanced CH_3 asymmetric stretch around 2962 cm^{-1}, which can be assigned to the *tert*-butyl groups of the hindered phenol antioxidant [18,26].

X-ray photoelectron spectroscopy (XPS) technique is more surface sensitive than FT-IR and provides more information on the chemical nature of the surface species. The XPS measurement was performed to compare the N1s binding energy in AEAPS–silica and AO–AEAPS–silica. The chemical atmosphere of –NH– groups is similar to that of $-NH_2$ groups in the structure of AEAPS–silica. Hence, the peaks of –NH– groups are overlapped with that of $-NH_2$ groups. In AEAPS–silica (Fig. 2a), the N1s spectrum shows an intense peak at 399.2 eV and a weak shoulder peak at 400.9 eV. The low binding energy originates from the free amines (–NH– and $-NH_2$) and the high binding energy comes from the protonated amines ($-NH_2^+$ and $-NH_3^+$). In AO–AEAPS–silica (Fig. 2b), two signals could be resolved at binding energies of 399.9 eV and 401.7 eV. The low binding energy 399.9 eV was attributed to the characteristic of –NH– or residual $-NH_2$ groups [21,27,28]. The high binding energy was assigned to the amide (–NH–(C=O)–) characteristic in AO–AEAPS–silica. Therefore, the XPS results further confirmed that the reactive antioxidant was chemically immobilized onto the surface of nanosilica particles through the $-NH_2$ groups of AEAPS anchored on nanosilica.

The results of the thermogravimetric analysis (TGA) of neat nanosilica and modified nanosilica are presented in Fig. 3. The stoichiometry of the reaction AO–AEAPS is 1:1, as shown in Scheme 1. Based on the weight losses of AEAPS–silica and AO–AEAPS–silica from 200 °C to 750 °C, the loading of antioxidant on the AO–AEAPS–silica is 10.22 wt%, corresponding to 0.39 mmol antioxidant per 1 g AO–AEAPS–silica.

3.2. Morphology and dispersion of nanosilica

The morphologies of nanosilica before and after modification have been investigated by TEM observations, as shown in Fig. 4. It is observed that the aggregation of neat nanosilica is largely reduced after surface modified with the aminosilane coupling agent AEAPS and successively reacted with the reactive antioxidant. The neat nanosilica tends to form large aggregates and agglomerates because of the formation of hydrogen band between the abundant hydroxyl groups and adsorbed

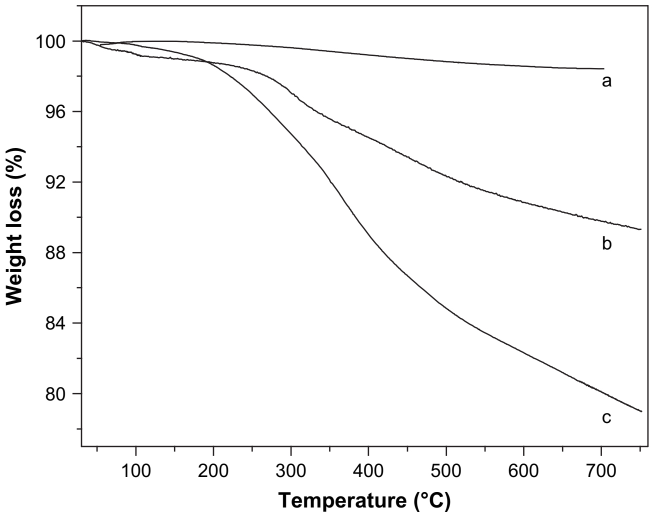

Fig. 3. The TG curves of (a) neat nanosilica, (b) AEAPS–silica and (c) AO–AEAPS–silica.

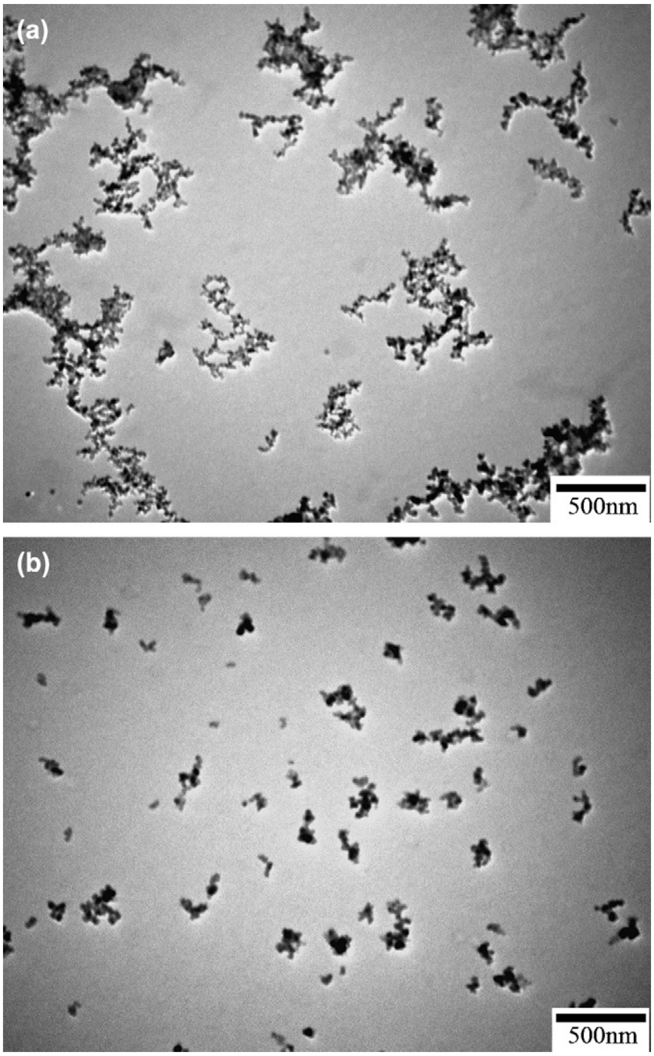

Fig. 4. TEM images of (a) neat nanosilica and (b) AO–AEAPS–silica.

water on their surface. After modification, most of hydroxyl groups have been reacted and antioxidant molecules covered the nanosilica surface. Then, the surface have turned from hydrophilic to hydrophobic, more compatible with the apolar polymer matrix, and thus reduced the aggregation of the nanoparticles.

The dispersion states of neat nanosilica and AO–AEAPS–silica in low density polyethylene were evaluated in SEM observations. Fig. 5a and b shows the SEM images of LDPE/nanosilica and LDPE/AO–AEAPS–silica nanocomposites, respectively. It was found that the neat nanosilica was nonuniformly dispersed in LDPE matrix as large aggregates and agglomerates. On the contrary, the AO–AEAPS–silica was well-dispersed in LDPE matrix. The reactive antioxidant has been immobilized onto the nanosilica surface. The antioxidative efficiency is related to the dispersion state of antioxidant in polyolefins. Hence, the homogenous dispersion of AO–AEAPS–silica will be effective to prevent the thermal oxidative degradation of low density polyethylene.

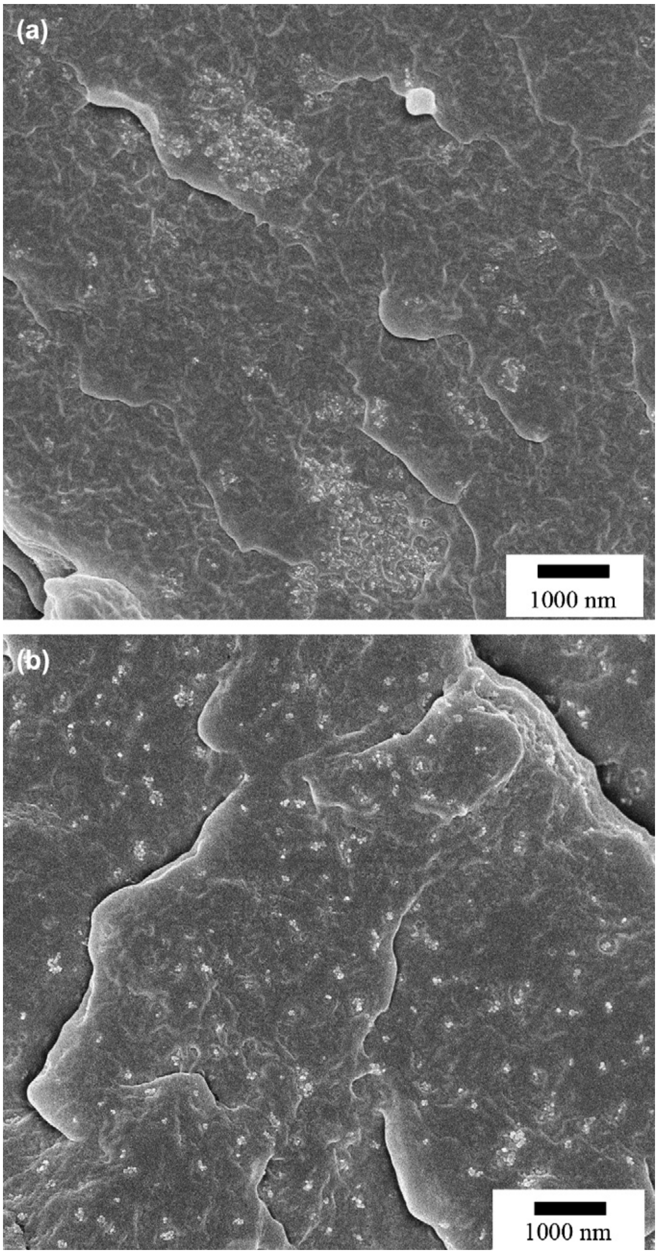

Fig. 5. SEM images of (a) LDPE/nanosilica and (b) LDPE/AO–AEAPS–silica nanocomposites.

3.3. The thermal oxidative degradation of LDPE/silica nanocomposites

The antioxidant molecules in the AO–AEAPS–silica are chemically immobilized and less migratory than the original ones. Therefore, AO–AEAPS–silica could be utilized as an antioxidant for polyolefins. Several LDPE compounds were prepared and their antioxidative behavior was evaluated by oxidation induction time (OIT) method. OIT is the time interval between the initiation of oxygen flow and the onset of the oxidative reaction in the DSC testing. The more resistant the sample is to oxidative degradation, the longer the OIT value is. In all nanosilica-containing samples, the content of inorganic component was fixed at 4 wt% in order to eliminate the effect

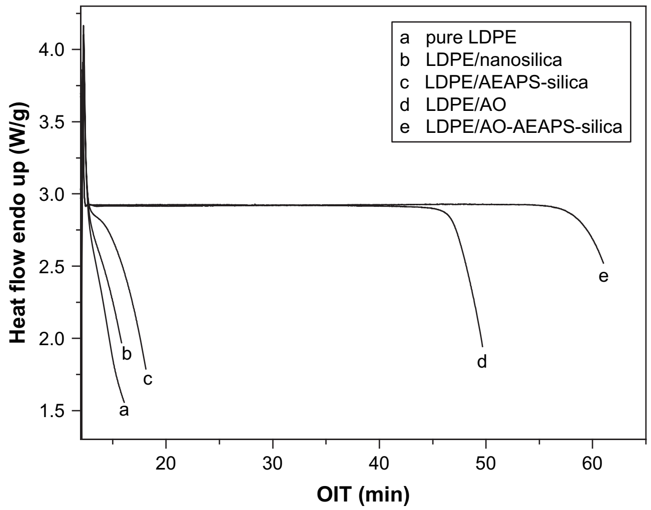

Fig. 6. Determination of OIT (DSC measurement, 200 °C).

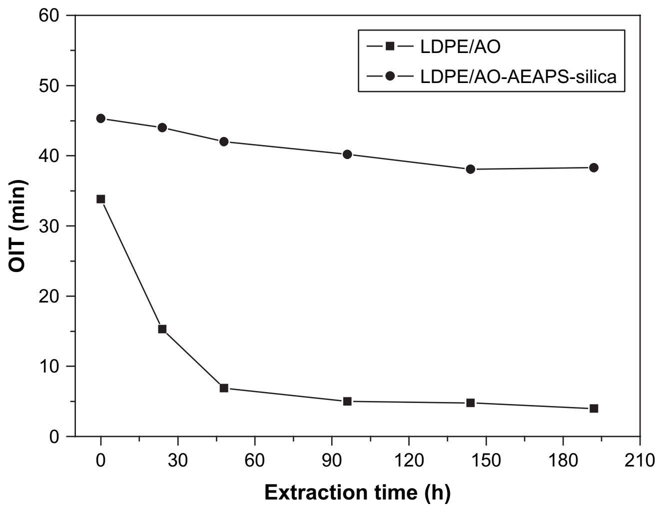

Fig. 7. OIT versus extraction time of LDPE/AO and LDPE/AO–AEAPS–silica compounds.

of neat nanosilica on the OIT values of LDPE compounds. According to the DSC curves (Fig. 6), it was showed that the pure LDPE and LDPE/nanosilica composites almost immediately turn to the stage of oxidative degradation under the oxygen atmosphere at 200 °C. It indicates that the neat nanosilica had no contribution to the OIT values of LDPE nanocomposites. Table 2 shows the OIT values of the several LDPE compounds. The OIT value of LDPE/AEAPS–silica (3 min) is slightly higher than that of pure LDPE (1 min). This result indicates that aminosilane coupling agent had little effect on thermal oxidative stability of low density polyethylene. The AO–AEAPS–silica, which contained the antioxidant molecules, was incorporated into LDPE matrix. The OIT value of LDPE/AO–AEAPS–silica is 45.3 min, much higher than those of pure LDPE, LDPE/nanosilica and LDPE/AEAPS–silica compounds. The above results revealed that the AO–AEAPS–silica was much more efficient than neat nanosilica and AEAPS–silica in preventing thermal oxidative degradation of LDPE nanocomposites. It was obvious that the phenol hydroxyl of the AO–AEAPS–silica was most responsible for the exceptional antioxidative behavior. As a reference, the OIT value of the LDPE/AO, containing equivalent antioxidant in LDPE/AO–AEAPS–silica, is only 33.8 min, which is 11.5 min shorter than that of LDPE/AO–AEAPS–silica. One reason for the shorter OIT of LDPE/AO compound could be the volatilization of antioxidant during the melt compounding because of its low molecular weight. That is to say, the antioxidant molecules immobilized onto nanosilica surface was not easy to volatilize at high temperatures.

A second way to evaluate the antioxidative efficiency is the comparison of OIT change of the samples upon solvent extraction, as shown in Fig. 7. The OIT value of LDPE/AO sharply reduced to 6.9 min from 33.8 min (ca. 80% reduction) after extraction in de-ionized water at 45 °C for 48 h. It indicated that the low molecular antioxidant can easily migrate from LDPE matrix to the surrounding water. On the contrary, the OIT values of LDPE/AO–AEAPS–silica before and after extraction for 192 h reveal no significant difference, with a reduction of only ~10%. It was obvious that the antioxidant immobilized onto the nanosilica surface was much more effective than the corresponding low molecular counterpart, especially in the presence of extractive solvent environment.

Table 2
OIT values obtained by DSC measurement at 200 °C

Sample	LDPE	LDPE/ nanosilica	LDPE/ AEAPS–silica	LDPE/AO	LDPE/AO– AEAPS–silica
OIT (min)	1.0	1.2	3.0	33.8	45.3

4. Conclusions

In this paper, we have demonstrated for the first time that nanosilica could be utilized as an appropriate support for immobilization of antioxidant molecules. The reactive antioxidant was successfully immobilized onto the surface of nanosilica particles via the aminosilane coupling agent, which has been conformed by several measurements. This nanosilica-immobilized antioxidant was homogeneously dispersed in the matrix of low density polyethylene and showed improved antioxidative efficiency in the nanocomposite compared to the corresponding low molecular counterpart. It has been revealed that the nanosilica-immobilized antioxidant retained excellent stability in LDPE matrix against water extraction.

Acknowledgments

This work was financially supported by the National Natural Science Foundation of China (Grant No. 50473054 and 50533070) and the Major Basic Research Projects of China (Grant 003CB615600).

References

[1] Bertoldo M, Ciardelli F. Polymer 2004;45:8751–9.
[2] Kim TH, Oh DR. Polym Degrad Stab 2004;84:499–503.
[3] Haider N, Karlsson S. Biomacromolecules 2000;1:481–7.

[4] Al-Malaika S, Golovoy A, Wilkie CA. Chemistry and technology of polymer additives. Blackwell Science; 1999.

[5] Bergenudd H, Eriksson P, DeArmitt C, Stenberg B, Jonsson EM. Polym Degrad Stab 2002;76:503–9.

[6] Kontou E, Niaounakis M. Polymer 2006;47:1267–80.

[7] Wu CL, Zhang MQ, Rong MZ, Friedrich K. Compos Sci Technol 2002;62:1327–40.

[8] Landry CJT, Coltrain BK, Brady BK. Polymer 1992;33:1486–95.

[9] Ji XL, Hampsey JE, Hu QY, He JB, Yang ZZ, Lu YF. Chem Mater 2003;15:3656–62.

[10] Cheng CF, Cheng HH, Cheng PW, Lee YJ. Macromolecules 2006;39: 7583–90.

[11] Luo J, Wang XH, Li J, Zhao XJ, Wang FS. Polymer 2007;48:4368–74.

[12] Hu YH, Chen CY, Wang CC. Polym Degrad Stab 2004;84:545–53.

[13] Hou ZJJ, Liu LYY, Xu L, Xu ZLL, Wang WCC, Li FMM, et al. Chem Mater 1999;11:3177–80.

[14] Liu CH, Pan CY. Polymer 2007;48:3679–85.

[15] Peng HS, Tang J, Yang L, Pang JB, Ashbaugh HS, Brinker CJ, et al. J Am Chem Soc (Commun) 2006;128:5304–5.

[16] Paul DR, Takahashi S. Polymer 2006;47:7535–47.

[17] Shang XY, Zhu ZK, Yin J, Ma XD. Chem Mater 2002;14:71–7.

[18] Jin L, Horgan A, Levicky R. Langmuir 2003;19:6968–75.

[19] Blin JL, Gérardin C, Rodehüser L, Selve C, Stébé MJ. Chem Mater 2004;16:5071–80.

[20] Corrie SR, Lawrie GA, Trau M. Langmuir 2006;22:2731–7.

[21] Li HL, Perkas N, Li QL, Gofer Y, Koltypin Y, Gedanken A. Langmuir 2003;19:10409–13.

[22] Britcher L, Rahiala H, Hakala K, Mikkola P, Rosenholm JB. Chem Mater 2004;16:5713–20.

[23] Roveda C, Church TL, Alper H, Scott SL. Chem Mater 2000;12: 857–62.

[24] Lee BY, Oh JS. Macromolecules 2000;33:3194–5.

[25] Budny A, Novak F, Plumeré N, Schetter B, Speiser B, Straub D, et al. Langmuir 2006;22:10605–11.

[26] Seman M, Kondo JN, Domen K, Radhakrishnan R, Oyama ST. J Phys Chem B 2002;106:12965–77.

[27] Kallury KMR, Krull UJ, Thompson M. Anal Chem 1988;60: 169–72.

[28] Saprigin AV, Thomas CW, Dulcey CS, Patterson CH, Spector MS. Surf Interface Anal 2004;36:24–32.